Available online at www.sciencedirect.com
ScienceDirect
Journal of Molecular Graphics and Modelling 26 (2008) 1365–1369
Journal of Molecular Graphics and Modelling
www.elsevier.com/locate/JMGM

Molecular modeling optimization of anticoagulant pyridine derivatives

Jose A. Hernandez Prada [b], Sandra L. Madden [a], David A. Ostrov [b], Maria A. Hernandez [a,*]

[a] College of Pharmacy, Nova Southeastern University, Ft. Lauderdale, FL, USA
[b] University of Florida, Department of Pathology, Immunology and Laboratory Medicine, College of Medicine, Gainesville, FL, USA

Received 8 August 2007; received in revised form 25 January 2008; accepted 26 January 2008
Available online 7 February 2008

Abstract

Intravascular clotting remains a major health problem in the United States, the most prominent being deep vein thrombosis, pulmonary embolism and thromboembolic stroke. Previous reports on the use of pyridine derivatives in cardiovascular drug development encourage us to pursue new types of compounds based on a pyridine scaffold. Eleven pyridine derivatives (oximes, semicarbazones, N-oxides) previously synthesized in our laboratories were tested as anticoagulants on pooled normal plasma using the prothrombin time (PT) protocol. The best anticoagulant within the oxime series was compound AF4, within the oxime N-oxide series was compound AF4-N-oxide, and within the semicarbazone series, compound MD1-30Y. We also used a molecular modeling approach to guide our efforts, and found that there was good correlation between coagulation data and computational energy scores. Molecular docking was performed to target the active site of thrombin with the DOCK v5.2 package. The results of molecular modeling indicate that improvement in anticoagulant activities can be expected by functionalization at the three-position of the pyridine ring and by N-oxide formation. Results reported here prove the suitability of DOCK in the lead optimization process.

Keywords: Pyridine oximes; Pyridine semicarbazones; Anticoagulants; Molecular modeling; DOCK; Thrombin

1. Introduction

A major cause of mortality and morbidity in the western world are the thromboembolic disorders resulting from excessive activation of the coagulation cascade. The most prominent of such adverse intravascular clotting events include deep vein thrombosis (DVT), pulmonary embolism (PE) and thromboembolic stroke [1]. The blood coagulation system consists of a number of inactive enzymes (zymogens) that are activated in a cascade of enzymatic reactions. The final step in coagulation is the formation of the fibrin clot from fibrinogen, by the action of the serine protease thrombin, which in turn is generated from prothrombin by the action of factor Xa.

Direct thrombin inhibitors (DTI) have been the focus of intense research and offer the advantage of binding directly to fibrin-bound thrombin, in addition to being orally bioavailable. Thus, DTIs offer an alternative to the more traditional anticoagulant therapies of vitamin K antagonists (e.g. Warfarin), and other thrombin inhibitors that must be administered parenterally (Lepirudin) [2,3]. A disadvantage of vitamin K antagonists is that many have undesirable drug interactions and need close monitoring of blood coagulation parameters. Recently, the direct thrombin inhibitor Ximelagatran (Melagatran's prodrug) was removed from the market by its manufacturer due to liver toxicities [4], leaving a need for newer and safer DTIs to be developed. Previous studies on thrombin inhibitors that can be developed into new anticoagulant drugs involved the use of the isocoumarin scaffold [5,6]. These derivatives, however, were irreversible inhibitors that did not progress beyond animal testing due to excessive bleeding [7]. Other reports on the use of pyridine derivatives in drug development [8–10] encourage us to pursue new types of compounds based on a pyridine scaffold, using molecular modeling techniques to guide synthesis and biochemical testing. The program DOCKv5.12 [11] allows the identification of low-energy binding modes of small molecules (ligands) within the active site of a macromolecule, the enzyme thrombin in this case.

We report here on the effectiveness of eleven pyridine oxime and semicarbazone derivatives in increasing the coagulation

* Corresponding author at: College of Pharmacy, Nova Southeastern University, Terry Building, Room 1350, 3200 S. University Dr., Ft. Lauderdale, FL 33328, USA. Tel.: +1 954 262 1350; fax: +1 954 262 2278.
E-mail address: Mariah@nova.edu (M.A. Hernandez).

1093-3263/$ – see front matter © 2008 Elsevier Inc. All rights reserved.
doi:10.1016/j.jmgm.2008.01.006

time of human plasma, analyze molecular docking results of the pyridine derivatives and describe future plans for drug development in this family of compounds. Surprisingly, we observe a correlation between *in vitro* and predicted activity of these compounds which encourages us to suggest that molecular docking may be particularly useful for the development of novel anticoagulants derived from this system.

2. Materials and methods

Chemical synthesis of pyridine derivatives was performed as reported in our patents [8,9], by reacting a commercially available aldehyde with a suitable hydroxylamine or semicarbazide. If not commercially available, the aldehyde was prepared by oxidation of the aliphatic alcohol with manganese dioxide. The N-oxides were prepared by standard methodology, in a chloroform solution of *m*-chloroperbenzoic acid (*m*-CPBA). Chemical reagents and solvents were purchased through VWR Scientific or Aldrich Chemical Company.

Anticoagulant testing was performed on the BBL Fibrometer [12]. This instrument automatically detects fibrin clot formation. The CryoCheck Pooled Normal Plasma from PrecisionBioLogic, Dartmouth, NS, Canada was used as the human plasma reagent [13]. The protime (PT) reagent was Simplastin HTF manufactured by bioMérieux Inc., Durham, NC. The refrigerated reagent was warmed to 37 °C in the fibrometer for 5 min prior to use. A reaction cup was placed in the fibrometer, then 100 μL of test plasma was pipetted into the cup and warmed for 3 min. Simultaneously, 200 μL of thromboplastin reagent was pipetted into the fibrocup as the timer was depressed. The clotting time in seconds was recorded from the timer [14]. Results are shown in Table 1. The structures of the pyridine derivatives developed and tested as anticoagulants are shown in Fig. 1.

Molecular modeling and docking of the pyridine derivative interactions were performed using the crystal structure of thrombin available through the Protein Data Bank (PDB code: 1SL3, [15]). Water molecules and other heteroatoms were deleted from the thrombin structure before docking. A virtual library of the pyridine derivatives was generated through ZINC [16] to accurately assign partial charges to each compound and obtain appropriately formatted coordinate files. Molecular docking was performed to target the active site of thrombin with the DOCK v5.2 package [11], which generates spheres to map the cavity in the active site (Fig. 2A). DOCK matches each pyridine derivative to these spheres in an attempt to ''pose'' the ligand in the unoccupied space available. Orientations meeting matching criteria (to avoid steric clashes, for example) are identified and submitted to the minimization routines in DOCK v5.12. The modeled complex is optimized to increase favorable molecular interactions. In addition, each compound was treated as a flexible ligand, which allows searching the conformational space of each compound within the active site of thrombin. Molecular interactions are evaluated by calculating approximate molecular mechanics interaction energies as implemented by the force field function in DOCK v5.12:

$$E = \sum_{i=1}^{\text{lig}} \sum_{j=1}^{\text{rec}} \left(\frac{A_{ij}}{r_{ij}^{a}} - \frac{B_{ij}}{r_{ij}^{b}} + 332 \frac{q_i q_j}{D r_{ij}} \right)$$

This scoring function includes Van der Waals and electrostatic terms. The atoms of thrombin included in this calculation are delimited by the site ''box'' (see Fig. 2).

3. Results and discussion

In silico molecular docking was performed using increasingly thorough searches with DOCK until the DOCK energy scores converged and did not improve any further. Table 1 shows the prothrombin times (PT, in seconds) of the pyridine derivatives alongside with the binding scores obtained using DOCK. The results clearly indicate a direct correlation between DOCK binding scores and the anticoagulant activity of the pyridine derivatives. It is likely that these data will be also correlated to binding interactions and hydrogen bonding networks between the compounds and the active site. However, accurate crystal structures will be required for a more detailed analysis of specific binding interactions.

Coagulation times reported in Table 1 are average results of duplicate experiments and represent a 10–15% increase in the coagulation time of pooled normal plasma used as control. The concentrations of the pyridine derivatives were in the range of

Table 1
Coagulation times and DOCK energy scores of pyridine derivatives

Compound	Pyridine semicarbazones	DOCK energy score	Coagulation time (PT, s)
MD1-30Y	4-Amino-*N*-[(3-hydroxy-6-methyl-2-pyridyl)methyleneamino] benzamide	−38.7	14.2
MD1-30W	4-Amino-*N*-(4-pyridylmethyl eneamino) benzamide	−36.2	12.9
MD1-29Y	4-Amino-benzoic acid pyridin-3-ylmethylene-hydrazide	Not determined	12.7
MD1-14Y	1-Amino-*N*-[(3-hydroxy-6-methyl-2-pyridyl)methyleneamino] formamide	−32.7	12.2
MD1-29W	4-Amino-*N*-(2-pyridylmethylene amino) benzamide	−34.8	11.9

Compound	Pyridine oximes and N-oxides	DOCK energy score	Coagulation time (PT, s)
AF4-NO	4-[(4-Nitrophenyl)methoxyimino methyl]-1H-pyridin-1-ol	−40.5	14.5
AF3-NO	3-[(4-Nitrophenyl)methoxyimino methyl]-1H-pyridin-1-ol	−37.8	14.4
AF2-NO	2-[(4-Nitrophenyl)methoxyimino methyl]-1H-pyridin-1-ol	−37.5	14.2
AF4	*N*-[(4-Nitrophenyl)methoxy]-1-(4-pyridyl)methanimine	−37.8	12.0
AF3	*N*-[(4-Nitrophenyl)methoxy]-1-(3-pyridyl)methanimine	−37.1	12.0
AF2	*N*-[(4-Nitrophenyl)methoxy]-1-(2-pyridyl)methanimine	−36.4	11.8

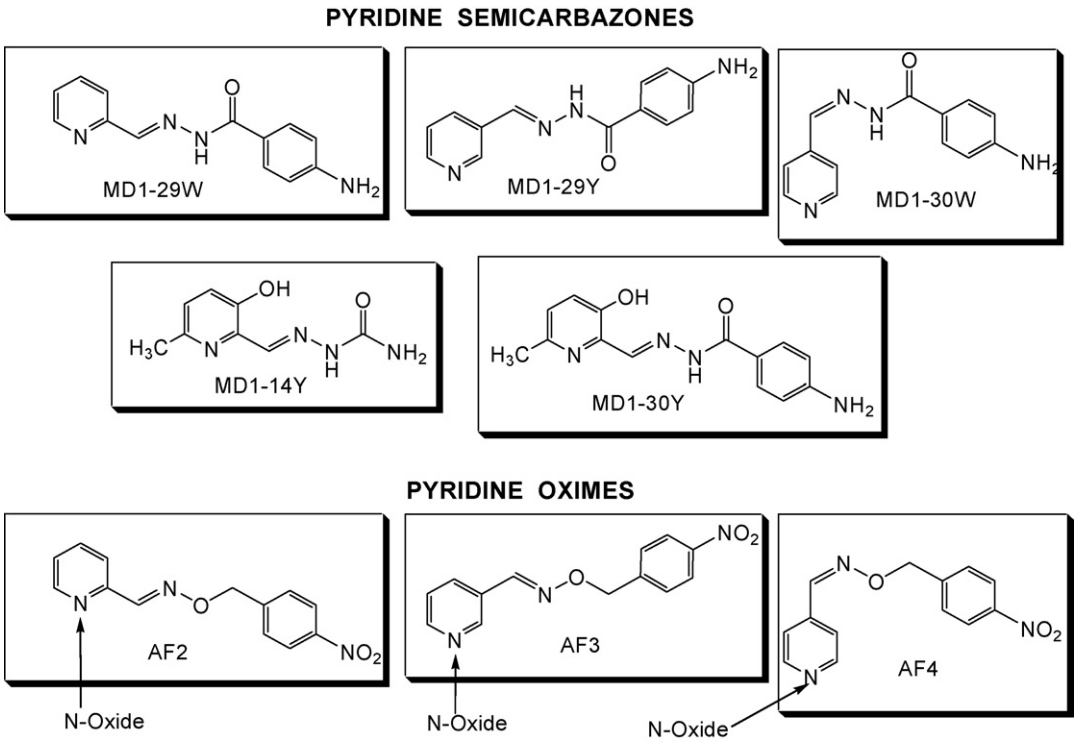

Fig. 1. Structures of pyridine derivatives. Derivatives were synthesized and prepared from aldehyde precursors and a semicarbazide or hydroxylamine derivative, as previously described [8,9]. *m*-Chloroperbenzoic acid was subsequently used to generate the N-oxide.

0.1–0.2 mM. The highest scoring pyridine oxime and semicarbazone derivatives are shown in Fig. 3A and B, respectively.

The best anticoagulant within the oxime series was compound AF4, within the oxime N-oxide series was compound AF4-N-oxide, and within the semicarbazone series, compound MD1-30Y. A comparative assessment of the binding of AF2, AF3, AF4 and their N-oxides indicates that maximum interactions and deeper reach into thrombin's active site are attained when there is a 1,4 relationship between the pyridine ring nitrogen and the oxime side chain. A hydrogen bond acceptor such as the nitro group or the N-oxide is preferred inside the active site; however, actual bond distance information to corroborate a hydrogen bonding network requires X-ray data, which is not within the scope of this publication.

A hydrophobic group (phenyl) at the two-position is preferred over an aliphatic chain (semicarbazone series) for

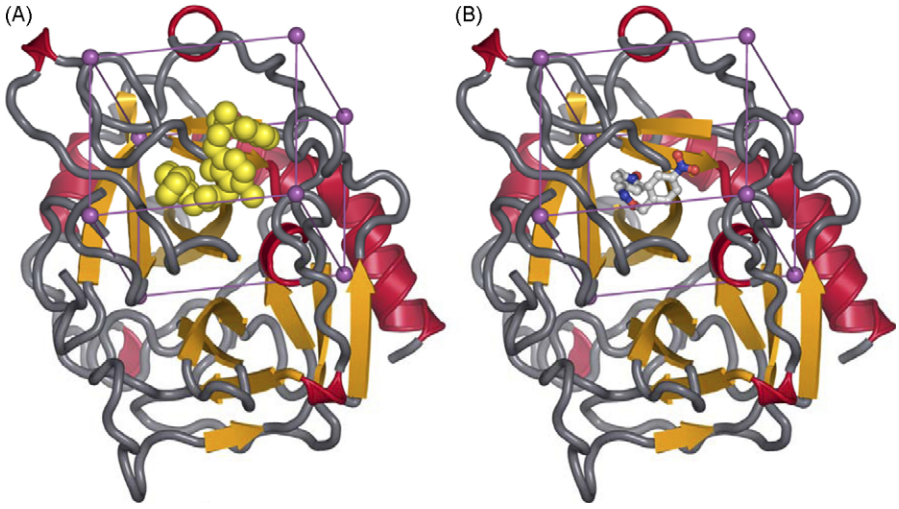

Fig. 2. Molecular docking. (A) Crystal structure of thrombin [15] (PDB ID: 1SL3) showing the spheres (in yellow) and scoring box (in purple) on which molecular interactions between pyridine derivatives and thrombin were calculated. The thrombin inhibitor in 1SL3 was omitted for the figure and docking calculations. Secondary structure colored in red (helices), gold (beta strands) and gray (coils). (B) Top scoring compound AF4-NO (see Table1) within the scoring box in the predicted binding orientation after analysis with DOCK [11]. Thrombin is colored and shown in identical orientation as in panel A. AF4-NO is colored according to elements (gray for carbon, red for oxygen, and blue for nitrogen).

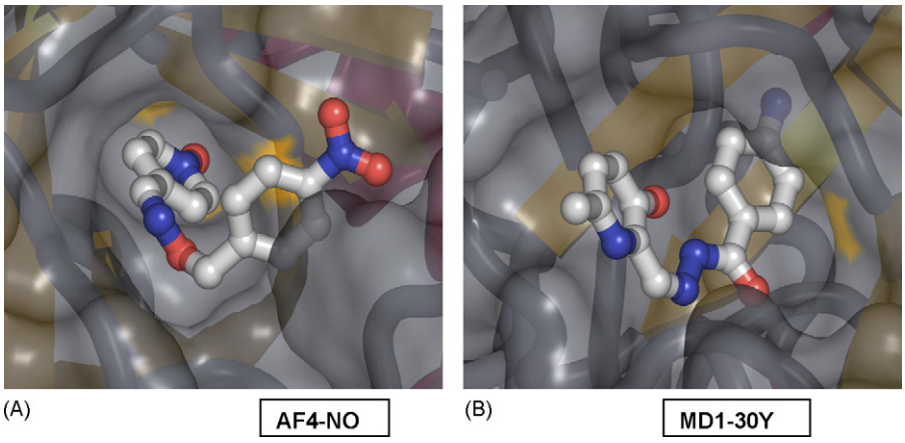

Fig. 3. Highest scoring pyridine oxime and semicarbazone. (A) Top scoring pyridine oxime (AF4-NO) in the active site of thrombin and in identical orientation to that of Fig. 2B. (B) Top scoring pyridine semicarbazone (MD1-30Y). Both panels show the molecular surface of thrombin at 20% transparency. Colored as in Fig. 2. Both figures made with pymol v0.98 [17].

anticoagulant activity (MD1-30Y versus MD1-14Y). This is reflected in the binding models for these compounds by an orientation in MD1-30Y that places the hydrogen bonding (phenyl)-NH_2 group far inside thrombin's active site, while in MD1-14Y neither the OH group nor the ring nitrogen are positioned inside the active site in a way that can lead to a productive hydrogen bond. The phenyl group in MD1-30Y favors a stronger interaction with the active site because there is 1,4 relationship between the NH_2 group and the side chain leading to the pyridine ring. In this way, the functional groups stretch out from the inner hydrogen bonding NH_2 to the semicarbazone unit and then to the pyridine ring.

The docking images generated by pymol for the compounds reported in Table 1 indicate that the OH group at the three position is important for binding (MD1-30Y versus MD-29W). This is reflected in the binding models for these compounds by the fact that the pyridine OH group is positioned outside the active site for MD1-30Y, in an orientation that is conducive to a hydrogen bond. On the other hand, the pyridine ring is inside the active site in MD1-29W, but the ring nitrogen is not positioned to have a productive hydrogen bond in this orientation, as is the case also for its (phenyl)-NH_2 group. Again, more accurate descriptions of hydrogen bonding networks can be achieved through evaluation of crystallographic X-ray data, which will be obtained with optimized compounds to be synthesized in the future.

4. Conclusions

Our results indicate that there was a direct correlation between coagulation data and binding scores generated by DOCK, which proves the suitability of DOCK's scoring function in the lead optimization process.

Improved anticoagulant activity will require building additional binding groups into the pyridine scaffold and derivatization into pyridine N-oxides. Within the oxime series, structural modifications suggested by these results include elongation and branching of the chain in AF4 and its N-oxide, to incorporate additional binding groups that can make productive contacts with thrombin's active site. Within the semicarbazone series, the most immediate changes suggested by these results include N-oxide formation at the pyridine ring, varying the position of the OH group in relation to the semicarbazone chain, and changing the position of the semicarbazone chain in relation to the pyridine ring nitrogen.

Future work using DOCK in our laboratories will involve virtual screening of several hundred pyridine derivatives and selection of the best scoring ones for synthesis and anticoagulant testing. The best inhibitor will then be crystallized with thrombin and X-ray data will be sought to clearly ascertain the hydrogen bonding network and the definitive orientation of the compound in the active site.

Acknowledgements

This work was supported by Nova Southeastern University under the Presidential Faculty Scholarship Award and by the University of Florida support from the National Institutes of Health (R21 HL080222) and the Cure Autism Now Foundation (2908051-12). We acknowledge Dr. John Irwin from the University of California for personally helping us obtain the virtual library from ZINC.

References

[1] M.V. Huisman, H. Bounameaux, Semin. Vasc. Med. 5 (2005) 276–284.
[2] M. Husmann, M. Barton, Expert Opin. Invest. Drugs 16 (2007) 563–567.
[3] M. Di Nisio, S. Middeldorp, H.R. Büller, N. Engl. J. Med. 353 (2005) 1028–1040.
[4] AstraZeneca, AstraZeneca decides to withdraw Exanta, February 14, 2006 Press release, Retrieved on 2007-07-02.
[5] C.M. Kam, J.E. Kerrigan, R.R. Plaskon, E.J. Duffy, P. Lollar, F.L. Suddath, J.C. Powers, J. Med. Chem. 37 (1994) 1298–1306.
[6] C.M. Kam, M.A. Hernandez, G.S. Patil, T. Ueda, W.H. Simmons, V.J. Braganza, J.C. Powers, Arch. Biochem. Biophys. 316 (1995) 808–814.
[7] Dr. Kam, personal communication.
[8] J.C. Powers, S.W. May, M.A. Hernandez, S.A. Thornton, J. Glinski, Quaternary Pyridinium Compounds, U.S. Patent No. 5,206,371, April 27, 1993.

[9] J.C. Powers, S.W. May, M.A. Hernandez, S.A. Thornton, J. Glinski, Quaternary Pyridinium Compounds and Uses Therefore, U.S. Patent No. 5,290,942, March 1, 1994.
[10] C.S. Burgey, K.A. Robinson, T.A. Lyle, P.E. Sanderson, S.D. Lewis, B.J. Lucas, J.A. Krueger, R. Singh, C. Miller-Stein, R.B. White, B. Wong, E.A. Lyle, P.D. Williams, C.A. Coburn, B.D. Dorsey, J.C. Barrow, M.T. Stranieri, M.A. Holahan, G.R. Sitko, J.J. Cook, D.R. McMasters, C.M. McDonough, W.M. Sanders, A.A. Wallace, F.C. Clayton, D. Bohn, Y.M. Leonard, T.J. Detwiler Jr, J.J. Lynch Jr, Y. Yan, Z. Chen, L. Kuo, S.J. Gardell, J.A. Shafer, J.P. Vacca, J. Med. Chem. 46 (2003) 461–473.
[11] T.J. Ewing, S. Makino, A.G. Skillman, I.D. Kuntz, J. Comput. Aided Mol. Des. 15 (5) (2001) 411–428.
[12] F. Lian, L. He, N. Colwell, P. Lollar, D. Tollefsen, Biochemistry 40 (2001) 8509.
[13] M. Bertina, F. Haverkate, J. Jespersen, Laboratory Techniques in Thrombosis—A Manual, Kluwer Academic Publishers, 1999, pp. 21–62.
[14] The BBL FibroSystem Manual, Becton Dickinson Microbiology Systems, fourth ed., April, 1992, pp. 1–52.
[15] M.B. Young, J.C. Barrow, K.L. Glass, G.F. Lundell, C.L. Newton, J.M. Pellicore, K.E. Rittle, H.G. Selnick, K.J. Stauffer, J.P. Vacca, P.D. Williams, D. Bohn, F.C. Clayton, J.J. Cook, J.A. Krueger, L.C. Kuo, S.D. Lewis, B.J. Lucas, D.R. McMasters, C. Miller-Stein, B.L. Pietrak, A.A. Wallace, R.B. White, B. Wong, Y. Yan, P.G. Nantermet, J. Med. Chem. 47 (2004) 2995–3008.
[16] J.J. Irwin, B.K. Shoichet, J. Chem. Inf. Model 45 (1) (2005) 177–182.
[17] W.L. DeLano, The PyMOL Molecular Graphics System, DeLano Scientific, San Carlos, CA, USA, 2002, http://www.pymol.org.